

Preparation of a New Crystal Form of Manganese Dioxide: λ - MnO_2

JAMES C. HUNTER

Union Carbide Corporation, P.O. Box 6116, Cleveland, Ohio 44101

Received January 12, 1981; in revised form March 9, 1981

Treatment of the spinel-type material LiMn_2O_4 with aqueous acid was found to result in conversion of the LiMn_2O_4 to nearly pure MnO_2 , while preserving the structural framework of the LiMn_2O_4 . The resulting material, designated λ - MnO_2 , thus has a structure related to spinel, but with most of the lithium removed from the tetrahedral sites. The conversion of LiMn_2O_4 to λ - MnO_2 results in some contraction of the lattice, as evidenced by a reduction in the lattice constant a_0 from 8.24 to 8.03 Å. A mechanism for the conversion of LiMn_2O_4 to λ - MnO_2 is proposed, which involves solid state diffusion of lithium in the structure, in a manner analogous to the proton diffusion which occurs during the cathodic reduction of γ - MnO_2 .

Introduction

MnO_2 and related manganese (IV) oxides are known to exist in a wide variety of structural forms. There are the materials β - MnO_2 (pyrolusite) and ramsdellite, which are relatively pure MnO_2 ; and others such as α - MnO_2 , δ - MnO_2 , γ - MnO_2 , etc., which contain significant amounts of other ions as integral parts of the structure.

The structural relationships between these various materials have been described by Wells (1) as well as in recent reviews by Burns and Burns (2, 3). The structures can be described in terms of octahedra composed of oxygen atoms with manganese atoms in the center. The various structural forms are then built up by linking these octahedra together in various ways.

For most of the MnO_2 materials, the structure can be described as consisting of parallel chains of edge-linked manganese-oxygen octahedra, linked together in various ways. Thus pyrolusite (β - MnO_2) con-

sists of single chains connected by corner sharing to other single chains. In ramsdellite there are double chains of octahedra, connected to other double chains by corner sharing. These two materials can also be viewed in terms of a distorted hexagonally close packed oxygen framework with manganese atoms placed in certain octahedral sites in the framework.

Other ways of joining together chains of manganese-oxygen octahedra give rise to α - MnO_2 (cryptomelane) and psilomelane. In these structures there are parallel tunnels which are large enough to contain other species, such as potassium, sodium, barium, or lead in the case of α - MnO_2 , and barium or potassium in the case of the psilomelane structure. In these structures, because of the large open tunnels present, the oxygen framework is not close packed.

δ - MnO_2 has a layer structure, with sheets made from manganese-oxygen octahedra, separated by alkali or other ions, and water. γ - MnO_2 , the material most commonly used as a cathode material in dry-cell bat-

teries, is considered to be a disordered intergrowth of the β - MnO_2 and ramsdellite structures (3), thus consisting of a random arrangement of single and double chains of MnO_6 octahedra.

There are some manganese (IV) containing compounds with structures based on a cubic closest packing (ccp) oxygen arrangement. Thus Li_2MnO_3 is proposed to have both lithium and manganese (IV) on octahedral sites in a ccp oxygen framework (4), while LiMn_2O_4 has the spinel structure, with lithium in tetrahedral sites and manganese (III) and manganese (IV) in octahedral sites of a ccp oxygen framework (5). In addition, some lower valent manganese compounds such as ZnMn_2O_4 and Mn_3O_4 are based on ccp or distorted ccp oxygen arrangements.

In the work reported here, it was discovered that one could convert the spinel structure, LiMn_2O_4 , to substantially pure MnO_2 while maintaining a structure derived from the spinel, i.e., with nearly all of the lithium removed from the tetrahedral sites, and with manganese remaining on the octahedral sites in the ccp oxygen framework.

Experimental

Synthesis of LiMn_2O_4 . LiMn_2O_4 was made as described by Wickham and Croft (5), by mixing appropriate amounts of Li_2CO_3 and a manganese oxide and heating at 850°C in air. Li_2CO_3 was Baker reagent grade. Manganese oxides used include Mn_2O_3 (98%) and Mn_3O_4 , from ALFA; and MnO (99%) from ROC/RIC.

Conversion of LiMn_2O_4 to λ - MnO_2 . For conversion of LiMn_2O_4 to λ - MnO_2 , a 15-g sample of LiMn_2O_4 was placed in a beaker containing 400 ml water, and a solution of dilute acid (H_2SO_4 , HNO_3 , or HCl) was added, with stirring, and while monitoring the solution pH. The solutions were stirred for approximately 45 min after the pH was stabilized at a particular value. Addition of

acid was halted at a series of solution pH values, to see the effect of solution pH on completeness of conversion. After the acid-treatment, the solution was then decanted and the remaining solid material washed by decantation, filtered in a sintered glass filter, and dried in air at 90°C .

Chemical analysis. Samples were analyzed for percentage of Mn and for manganese peroxidation using the ferrous sulfate–potassium permanganate titration method. Lithium content was determined using atomic absorption spectroscopy.

X-Ray diffraction. X-Ray powder diffraction analysis was performed using unfiltered $\text{FeK}\alpha$ radiation, or $\text{CuK}\alpha$ radiation (with a graphite monochromator), using a scintillation counter detector. In addition, unit cell dimensions of λ - MnO_2 were determined from high-angle X-ray diffraction data obtained using a Debye–Scherrer powder camera.

Thermal analysis. Thermal analyses were performed using a Dupont Model 950 thermogravimetric analyser and a Dupont Model 900 differential thermal analyzer with a differential scanning calorimeter (DSC) cell.

Results and Discussion

The synthesis of LiMn_2O_4 proceeded as described by Wickham and Croft (5), giving a blue powder with the proper X-ray pattern (ASTM card No. 18-736), and whose chemical analysis matched that expected for LiMn_2O_4 (see Table I). The solid state reaction between the Li_2CO_3 and manganese oxide proceeded rapidly, being largely complete in 1 hr, when the manganese oxide used was Mn_2O_3 . When lower valent oxides such as Mn_3O_4 were used, or when the amount of material was larger, longer heating times and multiple heatings were necessary to get complete reaction. (The solid state reaction to form LiMn_2O_4 was recently investigated by Schutte *et al.* (6).)

TABLE I
ANALYTICAL DATA FOR LiMn_2O_4 AND
ACID-TREATED LiMn_2O_4

Material	% Li	% Mn	% Peroxidation
LiMn_2O_4 theoretical	3.84	60.8	75
LiMn_2O_4 prepared as described	3.78	60.7	74.5
MnO_2 theoretical	0	63.2	100
Material from acid-treating LiMn_2O_4 at:			
pH 1	0.40	62.1	98
pH 2	0.46	62.2	97
pH 3	1.26	61.8	88
pH 4	2.48	61.6	84
pH 5	3.90	60.3	78.2

Treating the LiMn_2O_4 with a mildly acidic solution gave surprising results. After treating a sample with a solution of H_2SO_4 at pH2, a blue-black solid remained, yet there was a weight loss of approximately 29% from the starting LiMn_2O_4 to the final product. Analysis of the resulting material revealed that it was now a substantially pure manganese dioxide, with manganese peroxidation near 100% (i.e., manganese oxidation state near four), and with most of the lithium removed (See Table I).

Chemical analysis of the solution revealed that it contained the lithium that had been removed from the LiMn_2O_4 as well as the manganese, which was in the form of Mn^{2+} .

Even more surprising was the X-ray diffraction pattern of the resulting material. It had much the same pattern, in terms of relative line positions and intensities, as the LiMn_2O_4 , but with the lines shifted to slightly lower d values (Figs. 1a and b). Thus the pattern (with the exception of a weak line with a d value of 2.05 Å, attributed to some remaining LiMn_2O_4) could be indexed on a cubic unit cell, with lattice constant $a_0 = 8.03$ Å as compared to a lattice constant of 8.24 Å for LiMn_2O_4 (see Table II).

Since the X-ray scattering factors for manganese and oxygen are so much larger than for lithium, the diffraction pattern of

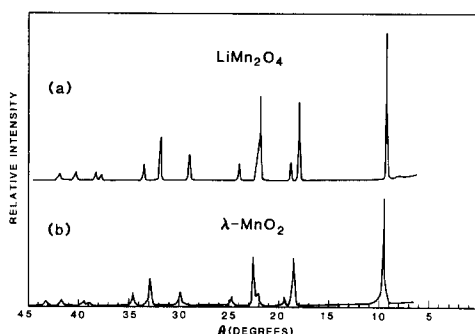


FIG. 1. X-Ray powder diffraction patterns ($\text{CuK}\alpha$ radiation) of (a) LiMn_2O_4 . (b) $\lambda\text{-MnO}_2$ resulting from pH 2 acid treatment of LiMn_2O_4 .

LiMn_2O_4 is due mainly to the manganese and oxygen atoms. The great similarity of this pattern to that of the acid-treated LiMn_2O_4 thus implies that the latter material has the same arrangement of manganese and oxygen atoms as in the spinel, but with a slightly smaller unit cell. From the X-ray data and the analytical results, therefore, it appears that acid treatment of LiMn_2O_4 leads to formation of a manganese dioxide of unique structure, derived from the spinel structure of LiMn_2O_4 but with most of the lithium removed from the tetrahedral sites. This material has been given the designation of $\lambda\text{-MnO}_2$.

This type of structure has been described

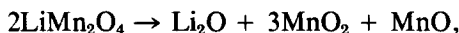
TABLE II
X-RAY DIFFRACTION DATA FOR LiMn_2O_4 AND
 $\lambda\text{-MnO}_2$

hkl	LiMn_2O_4 $d_{\text{obs}}(\text{ASTM 18-736})$	$\lambda\text{-MnO}_2$	
		d_{obs}	d_{calc}
111	4.72	4.64	4.636
311	2.47	2.42	2.421
222	2.37	2.31	2.318
400	2.05	2.01	2.008
331	1.88	1.84	1.842
333, 511	1.58	1.55	1.545
440	1.45	1.42	1.420
531	1.39	1.35	1.357

by A. F. Wells in his book, "Structural Inorganic Chemistry" (7). He notes that such a structure, related to spinel but with the tetrahedral sites vacant, is not adopted by any binary compound, although a distorted version of the structure is present in atacamite, $\text{Cu}_2(\text{OH})_3\text{Cl}$. He also notes that there are no apparent reasons that such a structure cannot exist for a binary compound. Apparently $\lambda\text{-MnO}_2$ is such a compound.

From the lattice constant of 8.03 Å, a density of 4.46 g/cm³ can be calculated for $\lambda\text{-MnO}_2$ compared to a measured value of 4.49 g/cm³.

A model has been developed to explain the conversion of LiMn_2O_4 to $\lambda\text{-MnO}_2$. The results of chemical analyses of the product and of the treating solution are consistent with the overall reaction:



where the lithium oxide and manganous oxides dissolve in the acidified treatment solutions. The real question is how this could occur without totally disrupting the LiMn_2O_4 structure. A dissolution-precipitation type mechanism is unlikely, since under the conditions of the acid treatment manganese is soluble only in the divalent state. The bulk of the manganese in LiMn_2O_4 would therefore be insoluble.

Conceivably, one could dissolve lithium oxide from the surface of the LiMn_2O_4 particles and also dissolve manganese (II) oxide (some disproportionation of $2\text{Mn(III)} \rightarrow \text{Mn(II)} + \text{Mn(IV)}$ at the surface would be needed). However, one would soon reach the point where the entire surface would consist of manganese (IV) oxide, and the conversion would stop. Since the conversion in fact does not stop, one must propose a model which effectively allows diffusion of lithium and manganese (III) through the bulk of the crystal. This can be done by invoking a mechanism somewhat analogous to that proposed by A. Kozawa and R. A.

Powers (8) for the cathodic reduction of $\gamma\text{-MnO}_2$ in alkaline electrolyte, but in reverse.

In the $\gamma\text{-MnO}_2$ reduction, the MnO_2 is reduced to MnOOH at the surface. The protons then diffuse to the interior of the particle, and electron hopping in the same direction occurs (Fig. 2a). This has the same effect as if the Mn(III) on the surface had diffused inward.

In the case of LiMn_2O_4 it can be thought of as analogous to $\gamma\text{-MnO}_2$ discharged to 0.5 electron equivalent. It consists of 50% Mn(III) and 50% Mn(IV) with Li^+ replacing H^+ . As the Li^+ and Mn^{2+} are removed from the surface by the acid solution, more lithium ions diffuse to the surface, accompanied by electron hopping (Fig. 2b). Thus, the dissolution can continue until all the lithium is removed and the manganese is all in the four-valent state. In all, 25% of the initial manganese will be removed from the surface of the particles; the interiors of the

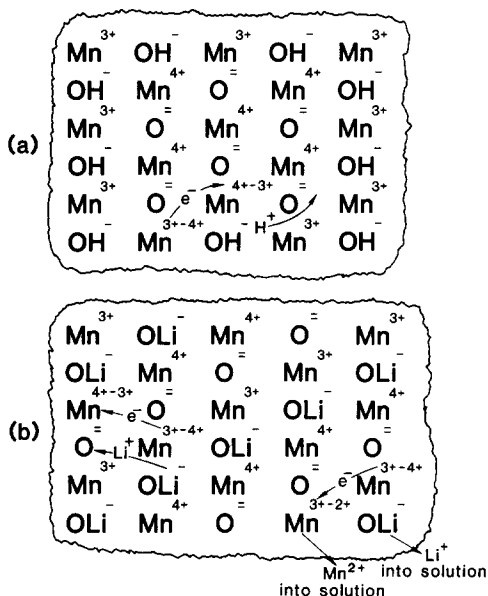


FIG. 2. Schematic representation of (a) equilibration of $\gamma\text{-MnO}_2$ particle during cathodic reduction, (b) conversion of LiMn_2O_4 to $\lambda\text{-MnO}_2$ in acidic aqueous solution.

particles will be left intact, though some contraction of the lattice will occur because of the loss of the lithium.

LiMn_2O_4 was treated with acid solutions under a variety of pH conditions. Analytical data for these samples are included in Table I. Conversion of LiMn_2O_4 to $\lambda\text{-MnO}_2$ is substantially complete when the pH of the treating solution is below approximately pH 2.5. Thus there was little difference seen between samples treated at pH 2 or 1. When LiMn_2O_4 is treated at higher pH's the conversion is incomplete. Above pH 5 very little conversion occurs. Even at a pH of 1 or 2 some lithium remains in the structure, and the manganese is not totally converted to the four-valent state. The reason for this inability to get complete conversion to a pure MnO_2 is not presently clear.

X-Ray diffraction data revealed that in the case of the partially converted LiMn_2O_4 there were peaks present due to both the LiMn_2O_4 and $\lambda\text{-MnO}_2$ structures. That is, the conversion did not proceed in a single phase with a gradual change in the lattice parameter, rather, it involved formation of separate regions of the $\lambda\text{-MnO}_2$ phase with the LiMn_2O_4 particles.

Thermogravimetric analysis of $\lambda\text{-MnO}_2$ in nitrogen atmosphere revealed little weight loss (<1%) occurring at temperatures up to 400°C. This behavior is qualitatively similar to that seen for pyrolusite ($\beta\text{-MnO}_2$) (9), although the amount of weight loss for $\lambda\text{-MnO}_2$ was somewhat higher than seen for $\beta\text{-MnO}_2$. In contrast, $\gamma\text{-MnO}_2$ is known to undergo a weight loss of several percent under the same conditions (10), largely due to loss of water from the structure.

Differential thermal analysis (DTA) results for $\gamma\text{-MnO}_2$ and $\beta\text{-MnO}_2$ have been reported in the literature (9, 10). In the case of $\beta\text{-MnO}_2$, an endothermic peak is seen in the temperature range of 500–600°C, corresponding to conversion of $\beta\text{-MnO}_2$ to

Mn_2O_3 . For $\gamma\text{-MnO}_2$ there is a broad endothermic region in the region from 100 to 400°C, corresponding to loss of water from the material, followed by a small exothermic peak at about 400°C corresponding to conversion to $\beta\text{-MnO}_2$, and then a large endothermic peak between 500 and 600°C corresponding to conversion to Mn_2O_3 . Differential scanning calorimeter (DSC) measurements on $\gamma\text{-MnO}_2$ and $\beta\text{-MnO}_2$ gave similar results to those reported in the literature.

DSC analysis of $\lambda\text{-MnO}_2$ gave results quite different from $\gamma\text{-MnO}_2$ or $\beta\text{-MnO}_2$. The $\lambda\text{-MnO}_2$ had a large exothermic peak at 258°C. The peak position was the same whether the DSC was performed in nitrogen or in air. An endothermic peak was found at 518°C in nitrogen and at 565°C in air.

The nature of the exothermic peak at 258°C was clarified by X-ray powder diffraction of $\lambda\text{-MnO}_2$ samples which were heated for 30 min in air at 200, 300, or 400°C, followed by cooling in air. The sample heated at 200°C still had the $\lambda\text{-MnO}_2$ pattern, while the sample heated at 300°C had the peaks of $\beta\text{-MnO}_2$, with very little of the $\lambda\text{-MnO}_2$ pattern remaining. For the 400°C material, the pattern was also that of $\beta\text{-MnO}_2$, with some improvement in the sharpness of the peaks. Thus the exothermic peak seen in the DSC analysis of $\lambda\text{-MnO}_2$ corresponds to conversion to $\beta\text{-MnO}_2$. The endothermic peak seen in the 500–600°C range is then the well-known $\beta\text{-MnO}_2 \rightarrow \text{Mn}_2\text{O}_3$ transition. Thus the evidence suggests that $\lambda\text{-MnO}_2$, like $\gamma\text{-MnO}_2$, is a metastable form of MnO_2 that, upon sufficient heating, reverts to the more stable $\beta\text{-MnO}_2$ form.

Acknowledgments

The author wishes to thank Dr. J. Akridge for performing X-ray diffraction analysis for determination of the lattice constant; Dr. J. A. van Lier and Mrs.

Kathy Maszczyński for performing thermal analysis work; and Mr. R. M. Estanek for assistance in preparation and chemical analysis of the materials.

References

1. A. F. WELLS, "Structural Inorganic Chemistry," 4th ed., pp. 468–481. Oxford Univ. Press, London (1975).
2. V. M. BURNS AND R. G. BURNS, "Manganese Dioxide Symposium," Vol. 1, Paper #15, p. 228. I. C. Sample Office, Cleveland (1975).
3. R. G. BURNS AND V. M. BURNS, "Manganese Dioxide Symposium," Vol. 1, Paper #16, p. 306. I. C. Sample Office, Cleveland (1975).
4. G. LANG, *Z. Anorg. Allg. Chem.* **348**, 246 (1966).
5. D. G. WICKHAM AND W. J. CROFT, *J. Phys. Chem. Solids* **7**, 351 (1958).
6. L. SCHUTTE, G. COLSMANN, AND B. REUTER, *J. Solid State Chem.* **27**, 227 (1979).
7. A. F. WELLS, "Structural Inorganic Chemistry," 4th ed. pp. 142–145, 268–269. Oxford Univ. Press, London (1975).
8. A. KOZAWA AND R. A. POWERS, *J. Electrochem. Soc.* **113**, 870 (1966).
9. J. P. BRENET, J. P. GABANO, AND M. SEIGNEURIN, "Proceedings, 16th International Conference of Pure and Applied Chemistry, Paris, 1957," Inorganic Chemistry Section, pp. 69–80.
10. D. M. TINSLEY AND J. H. SHARP, *J. Thermal Anal.* **3**, 43 (1971).